Arl4c is involved in tooth germ development through osteoblastic/ameloblastic differentiation

Thinh Thi Kim Truong
Laboratory of Oral Pathology, Division of Maxillofacial Diagnostic and Surgical Sciences, Faculty of Dental Science, Kyushu University

Fujii, Shinsuke
Laboratory of Oral Pathology, Division of Maxillofacial Diagnostic and Surgical Sciences, Faculty of Dental Science, Kyushu University

Nagano, Ryoko
Laboratory of Oral Pathology, Division of Maxillofacial Diagnostic and Surgical Sciences, Faculty of Dental Science, Kyushu University

Hasegawa, Kana
Laboratory of Oral Pathology, Division of Maxillofacial Diagnostic and Surgical Sciences, Faculty of Dental Science, Kyushu University

他

出版情報：Biochemical and Biophysical Research Communications. 679, pp.167-174, 2023-10-30. Elsevier
バージョン：

Arl4c is involved in tooth germ development through osteoblastic/ameloblastic differentiation

Thinh Thi Kim Truong[1], Shinsuke Fujii[1,2*], Ryoko Nagano[1,3], Kana Hasegawa[1], Megumi Kokura[1], Yuta Chiba[4], Keigo Yoshizaki[2,5], Satoshi Fukumoto[2,4,6] and Tamotsu Kiyoshima[1]

[1]Laboratory of Oral Pathology, Division of Maxillofacial Diagnostic and Surgical Sciences, Faculty of Dental Science, Kyushu University, 3-1-1 Maidashi, Higashi-ku, Fukuoka 812-8582, Japan

[2]Dento-craniofacial Development and Regeneration Research Center, Faculty of Dental Science, Kyushu University, 3-1-1 Maidashi, Higashi-ku, Fukuoka 812-8582, Japan

[3]Department of Endodontology and Operative Dentistry, Division of Oral Rehabilitation, Faculty of Dental Science, Kyushu University, 3-1-1 Maidashi, Higashi-ku, Fukuoka 812-8582, Japan

[4]Division of Pediatric Dentistry, Department of Oral Health and Development Sciences, Graduate School of Dentistry, Tohoku University Graduate School of Dentistry, 4-1 Seiryomachi, Aoba-ku, Sendai, 980-8575, Japan.

[5]Section of Orthodontics and Dentofacial Orthopedics, Division of Oral Health, Growth and Development, Faculty of Dental Science, Kyushu University, 3-1-1 Maidashi, Higashi-ku, Fukuoka 812-8582, Japan

[6]Section of Pediatric Dentistry and Special Need Dentistry, Division of Oral Health, Growth and Development, Faculty of Dental Science, Kyushu University, 3-1-1 Maidashi, Higashi-ku, Fukuoka 812-8582, Japan

*Corresponding author. Laboratory of Oral Pathology, Division of Maxillofacial Diagnostic and Surgical Sciences, Faculty of Dental Science, Kyushu University, 3-1-1 Maidashi, Higashi-ku, Fukuoka 812-8582, Japan

Phone: +81-92-642-6328; Fax: +81-92-642-6329

E-mail: sfujii@dent.kyushu-u.ac.jp

Keywords: Arl4c, Osteoblastic differentiation, Tooth germ development, Odontogenic epithelial cells

Abstract

Murine tooth germ development proceeds in continuous sequential steps with reciprocal interactions between the odontogenic epithelium and the adjacent mesenchyme, and several growth factor signaling pathways and their activation are required for tooth germ development. The expression of ADP-ribosylation factor (Arf)-like 4c (Arl4c) has been shown to induce cell proliferation, and is thereby involved in epithelial morphogenesis and tumorigenesis. In contrast, the other functions of Arl4c (in addition to cellular growth) are largely unknown. Although we recently demonstrated the involvement of the upregulated expression of Arl4c in the proliferation of ameloblastomas, which have the same origin as odontogenic epithelium, its effect on tooth germ development remains unclear. In the present study, single-cell RNA sequencing (scRNA-seq) analysis revealed that the expression of *Arl4c*, among 17 members of the Arf-family, was specifically detected in odontogenic epithelial cells, such as those of the stratum intermedium, stellate reticulum and outer enamel epithelium, of postnatal day 1 (P1) mouse molars. scRNA-seq analysis also demonstrated the higher expression of *Arl4c* in non-ameloblast and inner enamel epithelium, which include immature cells, of P7 mouse incisors. In the mouse tooth germ rudiment culture, treatment with SecinH3 (an inhibitor of the ARNO/Arf6 pathway) reduced the size, width and cusp height of the tooth germ and thickness of the eosinophilic layer, which would involve the synthesis of dentin and enamel matrix organization. In addition, loss-of-function experiments using siRNAs and shRNA revealed that the expression of Arl4c was involved in cell proliferation and osteoblastic cytodifferentiation in odontogenic epithelial cells. Finally, RNA-seq analysis with a gene set enrichment analysis (GSEA) and Gene Ontology (GO) analysis showed that osteoblastic differentiation-related gene sets and/or GO terms were downregulated in

shArl4c-expressing odontogenic epithelial cells. These results suggest that the Arl4c-ARNO/Arf6 pathway axis contributes to tooth germ development through osteoblastic/ameloblastic differentiation.

1. Introduction

Murine tooth germ development proceeds in continuous sequential steps with reciprocal interactions between the odontogenic epithelium and the adjacent mesenchyme, and several growth factor signaling pathways, including Wnt, bone morphogenetic proteins, fibroblast growth factors and sonic hedgehog pathways, and their signal activation are reported to be involved in tooth germ development, including the differentiation and proliferation stages [1].

ADP-ribosylation factor (Arf)-like proteins (Arls) are a subgroup of the ARF small GTP-binding protein superfamily [2,3]. Arl4c, a member of the Arl family proteins, is reported to be expressed in some epithelial rudiments, including tooth buds, hair follicles, salivary glands and kidneys, of embryonic day (E) 15 mouse embryos [4]. In addition, the particularly high expression of Arl4c in the distal tip of ureteric buds (UBs) of the mouse embryonic kidney has been shown to be involved in UB branching morphogenesis [4]. We recently demonstrated the involvement of the enhanced expression of Arl4c in the proliferation of ameloblastoma, which originates from the odontogenic epithelium [5]. Therefore, we hypothesized that Arl4c affects tooth germ development, but its effect on epithelial tooth bud morphogenesis remains unclear. In addition, recent reports describe the function of Arl4c, the expression of which is regulated by several mechanisms, including growth factor signaling, DNA methylation and microRNAs, to induce tumor cell proliferation [5-12]. However, the other functions of Arl4c (in addition to cell proliferation) are largely unknown.

Here, we investigated the expression patterns of Arl4c in the tooth germ at the single cell level and clarified the function of Arl4c in regulating cytodifferentiation using mouse tooth germ rudiment culture and cell lines.

2. Materials and methods

2.1. Cells and Reagents

mDE6 (mouse odontogenic epithelial cells) and SF2 (rat odontogenic epithelial cells) were used [13-15]. Lenti-X^{TM} 293T (X293T) cells were purchased from Takara Bio Inc. (Shiga, Japan). mDE6 cells and SF2 cells were cultured in DMEM/F12 (Thermo Fisher Scientific, Carlsbad, CA, USA) supplemented with 10% fetal bovine serum (FBS) (Thermo Fisher Scientific). X293T cells were grown in DMEM (Thermo Fisher Scientific) supplemented with 10% FBS. When necessary, the inhibitor, SecinH3 (TOCRIS Bioscience, Bristol, UK) was used.

For osteoblastic/ameloblastic differentiation experiments, mDE6 cells were plated in 24-well plates. At subconfluency, the cells were cultured in an osteoblastic/ameloblastic differentiation medium (DM) containing 50 μg/ml ascorbic acid (FUJIFILM Wako, Osaka, Japan) and 2 mM β-glycerophosphate (β-GP) (Sigma-Aldrich, St. Louis, MO, USA) [16,17]. The control medium (CM) and DM were changed every three days. After four weeks, the samples were fixed with 4% paraformaldehyde (PFA, Sigma-Aldrich) buffered by phosphate buffered saline (PBS) and stained with 1% Alizarin Red S (ALZ) (FUJIFILM Wako). The cells were viewed and the ALZ-positive area over the total area was analyzed by the All-in-one Fluorescence Microscope BZ 9000 (Keyence, Osaka, Japan).

2.2. Mouse tooth germ rudiments culture

Protocols used for all animal experiments in this study were approved by the Animal Research Committee of Kyushu University, Japan (No. A29-277-0, A21-065-0). E15 mouse tooth germ rudiments were cultured at an air-liquid interface on ThinCert^{TM} tissue

culture inserts with 1.0 μm pores (Greiner Bio-One, Berlin, Germany) in Fitton-Jackson's modified BGJb medium (Thermo Fisher Scientific) supplemented with 5% FBS, 100 μg/ml ascorbic acid (FUJIFILM Wako) and 100 unit/ml penicillin/streptomycin (Thermo Fisher Scientific) [14,18].

2.3. Single-cell RNA sequencing (scRNA-seq) analysis

In this study, the dataset, which was single-cell library preparation, sequencing, and data processing from postnatal day 1 (P1) molar and P7 incisor of Keratin14-RFP mice, was used [19,20].

2.4. Knockdown of protein expression by siRNA and quantitative RT-PCR

The effects of siRNA were analyzed as previously described [21]. In brief, siRNAs (final concentration 20 nM) were transfected into mDE6 and SF2 cells using Lipofectamine RNAiMAX (Thermo Fisher Scientific) and used for experiments 48 h post-transfection. Quantitative RT-PCR was performed as described previously [22]. Target sequences and primers are listed in Table S1 and S2.

2.5. Plasmid construction and infection using lentivirus harboring a cDNA or shRNA

To generate mDE6 cells that stably express GFP, Arl4c-GFP, shControl or shArl4c, parental cells (5×10^4 cells/well in a 12-well plate) were treated with lentivirus and 10 μg/ml polybrene [4,23]. The cells were then centrifuged at 1200 × g for 1 h, and incubated for another 24 h. The incubated cells with stable expression of GFP, Arl4c-GFP, shControl or shArl4c were selected and maintained in a culture medium containing 5 μg/ml Blasticidin S (FUJIFILM Wako) [24]. Target sequence for shArl4c is 5'-

GCAGGTCATTCTCTCGTAA-3'. Lentiviral vector was kindly provided by Dr. H. Miyoshi (RIKEN BioResource Center, Ibaraki, Japan) [25].

2.6. RNA sequencing and analyses

RNA-seq was performed using RNAs extracted from mDE6 cells expressing shControl or shArl4c. The sequencing libraries were prepared from 200 ng of total RNA with MGIEasy rRNA Depletion Kit and MGIEasy RNA Directional Library Prep Set (MGI Tech Co., Ltd. Shenzhen, China) according to the manufacturer's instructions. The libraries were sequenced on the DNBSEQ-G400 FAST Sequencer (MGI Tech Co., Ltd.) with the paired-end 150 nt strategy. All sequencing reads were trimmed low-quality bases and adapters with Trimmomatic (v.0.38) [26]. Raw counts for each gene were estimated in each sample using RSEM version 1.3.0 and Bowtie 2 [27,28]. We used edgeR program [29] to detect the differentially expressed genes (DEGs). Normalized counts per million (CPM) values, log fold-changes (logFC) and p-values were obtained from the gene-level raw counts. Then we established criteria for DEGs: p-value < 0.05 and ratio > 2 fold (up-regulated genes) or < 0.5 fold (down-regulated genes). The gene set enrichment analyses (GSEA) analysis with the Molecular Signature Database (v.7.2) was performed using the GSEA software (v.4.1.0) [30]. Gene Ontology (GO) analysis was performed using DAVID database (https://david-d.ncifcrf.gov) and summarized the data using REVIGO [31]. Data were deposited with the accession number GSE235460.

2.7. Immunohistochemistry staining

Mouse embryos at E15 and their tooth germ rudiments were collected, fixed in 4% PFA and processed for paraffin embedding. Then specimens were embedded in paraffin and sectioned at 5 μm thickness for H&E staining and immunohistochemical staining. Antigen retrieval (Dako, Carpentaria, CA, USA), elimination of the endogenous peroxidase activity (Dako), and blocking (Dako) were carried out as previously described [32,33]. Tissue sections were incubated with anti-Arl4c (HPA028927; Atlas antibodies, Voltavägen, SWE) (1:100) at 4°C overnight, and then the sections were incubated with secondary antibody (Histofine Simple Stain MAX PO, Nichirei, Tokyo, Japan) for 1 h at room temperature (RT). The immunoreactivity was visualized with DAB substrate solution (Nichirei). Subsequently, the sections were counterstained with hematoxylin.

2.8. Statistical analysis

Statistical analyses were performed using JMP Pro 16 software. Significant differences were determined using Student's *t*-test and one-way ANOVA with *post hoc* Tukey's test. A P value of <0.05 was considered to indicate statistical significance.

2.9. Additional Assays

Western blotting was performed as described previously [34] and data were representative of at least three independent experiments.

3. Results

3.1. The expression of Arl4c in the tooth germ

Consistent with a previous report [4], Arl4c was mainly expressed in the epithelium, especially in the stellate reticulum (SR), while Arl4c was hardly detected in the mesenchyme of the E15 mouse molar tooth germ, immunohistochemically (Supplementary Fig. S1A). In addition, E15 tooth germ rudiments were mechanically separated into the epithelium and mesenchyme, and then successful separation was confirmed by evaluating the expression of *Cadherin 1* (*Cdh1*) (epithelium marker) and *Vimentin* (mesenchyme marker) (Fig. 1A). Similar to the immunochemical results, the expression of *Arl4c* in the epithelium was higher than that in the mesenchyme (Fig. 1A).

Furthermore, to examine the expression pattern of *Arl4c* at the single-cell level, we used a dataset obtained from a scRNA-seq analysis of the P1 molars and P7 incisors of Keratin14-RFP mice, which were divided into 14 and 11 distinct clusters, respectively, using the Seurat v4 algorithm along with the expression patterns of specific genes, respectively (Supplementary Fig. S1B) [19,20]. Among the 17 members of the Arf-family members, the expression of *Arl4c* was specifically detected in the stratum intermedium (SI), SR-outer enamel epithelium (OEE) and leukocytes of the P1 molar (Fig. 1B; left panels). The abundant expression of *Arl4c* in SR-OEE appeared to be consistent with the immunohistochemistry data (Supplementary Fig. S1A). Additionally, a previous report demonstrated the elevated expression of *Arl4c* in thymic T-cell progenitors [35]. These results suggested that the current scRNA-seq data would be suitable for predicting the expression of *Arl4c*. In the P7 incisor, *Arl4c* was expressed in non-ameloblast and inner enamel epithelium (IEE), which are odontogenic epithelial cells of cervical loops that exhibit the characteristics of immature cells [36], but not in pre-ameloblasts or

ameloblasts (Fig. 1B; right panels). Therefore, we hypothesized that Arl4c might regulate the differentiation of odontogenic epithelial cells.

3.2. ARNO inhibition suppressed tooth germ development

The ARNO/Arf6 pathway could act downstream of Arl4c to regulate tube formation in intestinal epithelial cells [37] and cell proliferation in ameloblastoma cells, which originate from odontogenic epithelial cells [5]. In this study, we evaluated the involvement of the ARNO/Arf6 pathway in tooth germ development using organ culture of E15 mouse tooth germ rudiments. Because E15 tooth germ corresponds to the late cap stage in mouse tooth germ development, the cultured tooth germ rudiments would be likely to follow the developmental process of *in vivo* scenarios. In addition, tooth germ culture enables the investigation of the function of targeting specific genes/signaling pathways of interest [14,18].

Treatment with SecinH3 (an inhibitor of ARNO) significantly reduced the size, width and cusp height, but not the height, of tooth germ rudiments (Fig. 2A-C, and Supplementary Fig. S2A). Importantly, the thickness of the eosinophilic layer of the rudiments, which was observed between polarized ameloblasts and odontoblasts, was clearly decreased in SecinH3-treated groups in comparison to control groups (Fig. 2B, 2C and Supplementary Fig. S2B). These results suggested that the ARNO/Arf6 pathway may regulate tooth germ rudiment development, especially in the synthesis of dentin and enamel matrix organization. Next, we conducted a study to examine the direct effects of Arl4c on the differentiation of odontogenic epithelial cells using specific siRNA against Arl4c.

3.3. Arl4c regulated the expression of osteoblastic differentiation-related genes in odontogenic epithelial cells

First, we designed two different Arl4c siRNAs that would be effective in odontogenic epithelial cells such as mDE6 cells and SF2 cells (Supplementary Fig. S3A). Arl4c knockdown reduced the cell proliferation capabilities of both mDE6 cells and SF2 cells (Supplementary Fig. S3B). Lentiviral transduction with Arl4c rescued the siRNA-dependent decreases in the Arl4c protein expression and the reduction in mDE6 cell proliferation (Supplementary Fig. S3C). Cells expressing Arl4c showed proliferation capabilities similar to that of control mDE6 cells (Supplementary Fig. S3C). Because we used Arl4c #1 siRNA, which targets the 3'-UTR (untranslated region) (see Supplementary Table S1), it did not decrease the amount of exogenously expressed Arl4c-GFP in the cells, excluding the Arl4c #1 siRNA off-target in cell proliferation (Supplementary Fig. S3C). Next, the expression of specificity protein 7 (Sp7), also known as Osterix (Osx), which belongs to the zinc-finger-containing Sp1 family of transcription factors to induce the differentiation of osteoblasts, ameloblasts and odontoblasts [38,39], of mDE6 was higher than that of SF2, indicating that the osteoblastic/ameloblastic differentiation capabilities of mDE6 would be higher (Supplementary Fig. S3D). Therefore, we mainly used mDE6 cells in the following experiments on the induction of osteoblastic/ameloblastic differentiation.

Based on the above results using siRNAs, the target sequence of shArl4c was designed to be identical to that of Arl4c #1 siRNA and used in subsequent experiments. mDE6 cells stably expressing shArl4c were generated to constitutively reduce the levels of endogenous Arl4c (Fig. 3A). mDE6 cells expressing shControl or shArl4c were cultured in control medium (CM) or osteoblastic/ameloblastic differentiation medium

(DM) for 4 weeks. All cultures were then ALZ stained to observe the ALZ-positive small nodules in mDE6 cells expressing shControl but not in shArl4c-expressing or CM-cultured cells (Fig. 3B). These results suggested that the expression of Arl4c is involved in osteoblastic/ameloblastic differentiation in mDE6 cells.

Finally, to compare the molecular characteristics through which Arl4c affects cellular behaviors, RNA-seq analysis was performed in mDE6 expressing shControl and shArl4c. Volcano plot analyses revealed 1,629 and 1,127 downregulated and upregulated genes, respectively ($|\log2\text{-fold change}|<1$, $p<0.05$) (Fig. 3C). We further conducted GSEA (Fig. 3D), and GO analysis using DAVID database and summarized the data using REVIGO [31] (Supplementary Fig. S4). The gene sets “BONE MORPHOGENESIS”, “OSSIFICATION” and “OSTEOBLAST DIFFERENTIATION” were ranked as osteoblastic differentiation-related sets (Fig. 3D). TreeMap showed that a number of cellular functions were regulated by Arl4c, as shown in Supplementary Fig. S4A (downregulated group) and Supplementary Fig. S4B (upregulated group). Importantly, these analyses revealed that ossification, bone mineralization, positive regulation of bone mineralization and cell population proliferation were enriched in the downregulated group (Supplementary Fig. S4A), and the related genes（Supplementary Fig. S5) were found to be downregulated by quantitative RT-PCR (Fig. 3E). These results suggest that the expression of Arl4c could affect several behaviors in odontogenic epithelial cells.

4. Discussion

Recent reports have demonstrated that the expression of Arl4c is upregulated in tumors and associated with the progression of tumorigenesis, especially in the enhancement of proliferation capabilities [5-10,12]. In addition, Arl4c could be involved in mouse embryonic kidney development (e.g., UB branching morphogenesis). Organ formation by stem cells and tumor formation by tumor cells may share a common molecular mechanism [40], and accumulating evidence suggests that Arl4c would be raised as a candidate factor in the mechanism. In the current study, we clarified the function of Arl4c in the tooth germ development, demonstrating its involvement in differentiation.

The underlying mechanisms of Arl4c-dependent activation of Rac1-Arf6-yes-associated protein (YAP)/transcriptional co-activator with PDZ-binding motif (TAZ) signaling to regulate cell proliferation have been demonstrated in rat intestinal epithelial cells [4]. Arl4c induces the expression of genes, such as *phosphatidylinositol-3-kinase catalytic subunit delta isoform phosphatidylinositol-4,5-bisphosphate 3-kinase catalytic subunit delta* (*PIK3CD*), in hepatocellular carcinoma cells [8]. However, the mechanisms by which Arl4c, a member of the small G protein family, regulates the gene expression remain unclear. Consistently, the current RNA-seq analysis and RT-qPCR analysis indeed revealed that the expression of Arl4c could regulate the expression of large amounts of genes (see Fig. 3C). Among the genes, several GO terms related to osteoblast differentiation were downregulated in shArl4c-expressing mDE6 cells, which was consistent with decreased ALZ staining in the osteoblastic/ameloblastic differentiation culture. Since Arl4c is thought to affect unexpectedly diverse functions, an Arl4c knockout or transgenic mouse study is needed to clarify the precise function of Arl4c.

In tooth germ rudiment culture, treatment with SecinH3 reduced the thickness of the eosinophilic layer, which would involve the synthesis of dentin and enamel matrix organization. In addition, the size, width and cusp height of the rudiments in the SecinH3-treated groups were decreased in comparison to those in the control groups (see Fig. 2A-C and Supplementary Fig. S2A, S2B). These results suggested that ARNO/Arf6 pathway-dependent matrix organization would be important for aspects of tooth germ morphogenesis, such as size, width and cusp height. Meanwhile, the expression of *Arl4c* was lower in odontoblasts (see Fig. 1B), indicating that reciprocal interactions between the decreased function of the odontogenic epithelium with SecinH3 treatment and the adjacent mesenchyme might suppress dentin and enamel matrix organization.

Sp7 knockout mice exhibit small and misshapen teeth with randomly arranged cuboidal pre-odontoblasts and pre-ameloblasts with decreased markers of mature odontoblasts and ameloblasts, respectively [39]. Therefore, the decreased expression of Sp7 due to the inhibition of the Arl4c-ARNO/Arf6 pathway by SecinH3 (data not shown), would disorganize tooth germ development (see Fig. 2A-C). In shArl4c-expressing mDE6 cells, the expression of Sp7 was clearly downregulated. Sp7 is a downstream target of Runx2 [38]. In the current study, the knockdown of Arl4c with siRNA and shRNA reduced Sp7 but not Runx2 in odontogenic epithelial cells (data not shown). These data suggested that Arl4c could regulate the expression of Sp7, which might not be regulated by Runx2, at least in odontogenic epithelial cells. Therefore, further studies are needed to clarify the underlying mechanisms.

In summary, the specific expression of Arl4c in odontogenic epithelial cells induced osteoblastic/ameloblastic differentiation in tooth germ development. These

results suggest that the Arl4c-ARNO/Arf6 pathway axis contributes to tooth germ development.

Funding

This work was supported by JSPS KAKENHI Grant to S.F. (2023-2025; JP22KK0262), K.H. (2021-2023; JP21K09843) and T.K. (2023-2026; JP23H03102), Takeda Science Foundation, The Shinnihon Foundation of Advanced Medical Treatment Research, SGH Foundation, The Mochida Memorial Foundation for Medical and Pharmaceutical Research and TERUMO LIFE SCIENCE FOUNDATION to S.F., and Takeda Science Foundation and Fukuoka Public Health Promotion Organization Cancer Research Fund to K.H..

Declaration of competing interest

The authors declare that they have no known competing financial interests or personal relationships that could have appeared to influence the work reported in this paper.

Acknowledgments

The authors thank Drs. H. Wada, Y. Nakako and T. Fujimoto and appreciate the technical assistance from The Joint Use Laboratories, Faculty of Dental Science, Kyushu University.

References

[1] M. Jussila, I. Thesleff, Signaling networks regulating tooth organogenesis and regeneration, and the specification of dental mesenchymal and epithelial cell lineages, Cold Spring Harb. Perspect. Biol. 4 (2012) a008425. 10.1101/cshperspect.a008425.

[2] S. Matsumoto, S. Fujii, A. Kikuchi, Arl4c is a key regulator of tubulogenesis and tumourigenesis as a target gene of Wnt-β-catenin and growth factor-Ras signalling, J. Biochem. 161 (2017) 27-35. 10.1093/jb/mvw069.

[3] S. Fujii, T. Kiyoshima, The role of Wnt, ARL4C, and Sema3A in developmental process and disease pathogenesis, Pathol. Int. 73 (2023) 217-233. 10.1111/pin.13325.

[4] S. Matsumoto, S. Fujii, A. Sato, S. Ibuka, Y. Kagawa, M. Ishii, A. Kikuchi, A combination of Wnt and growth factor signaling induces Arl4c expression to form epithelial tubular structures, EMBO J. 33 (2014) 702-718. 10.1002/embj.201386942.

[5] S. Fujii, T. Ishibashi, M. Kokura, T. Fujimoto, S. Matsumoto, S. Shidara, K.J. Kurppa, J. Pape, J. Caton, P.R. Morgan, K. Heikinheimo, A. Kikuchi, E. Jimi, T. Kiyoshima, RAF1-MEK/ERK pathway-dependent ARL4C expression promotes ameloblastoma cell proliferation and osteoclast formation, J. Pathol. 256 (2022) 119-133. 10.1002/path.5814.

[6] S. Fujii, S. Matsumoto, S. Nojima, E. Morii, A. Kikuchi, Arl4c expression in colorectal and lung cancers promotes tumorigenesis and may represent a novel therapeutic target, Oncogene 34 (2015) 4834-4844. 10.1038/onc.2014.402.

[7] S. Fujii, K. Shinjo, S. Matsumoto, T. Harada, S. Nojima, S. Sato, Y. Usami, S. Toyosawa, E. Morii, Y. Kondo, A. Kikuchi, Epigenetic upregulation of ARL4C, due to DNA hypomethylation in the 3'-untranslated region, promotes tumorigenesis of lung squamous cell carcinoma, Oncotarget 7 (2016) 81571-81587. 10.18632/oncotarget.13147.

[8] T. Harada, S. Matsumoto, S. Hirota, H. Kimura, S. Fujii, Y. Kasahara, H. Gon, T. Yoshida, T. Itoh, N. Haraguchi, T. Mizushima, T. Noda, H. Eguchi, S. Nojima, E. Morii, T. Fukumoto, S. Obika, A. Kikuchi, Chemically Modified Antisense Oligonucleotide Against ARL4C Inhibits Primary and Metastatic Liver Tumor Growth, Mol. Cancer Ther. 18 (2019) 602-612. 10.1158/1535-7163.MCT-18-0824.

[9] K. Kimura, S. Matsumoto, T. Harada, E. Morii, I. Nagatomo, Y. Shintani, A. Kikuchi, ARL4C is associated with initiation and progression of lung adenocarcinoma and represents a therapeutic target, Cancer Sci. 111 (2020) 951-961. 10.1111/cas.14303.

[10] D.Z.R. Alkhatib, T. Thi Kim Truong, S. Fujii, K. Hasegawa, R. Nagano, Y. Tajiri, T. Kiyoshima, Stepwise activation of p63 and the MEK/ERK pathway induces the expression of ARL4C to promote oral squamous cell carcinoma cell proliferation, Pathol. Res. Pract. 246 (2023) 154493. 10.1016/j.prp.2023.154493.

[11] N. Xie, Y. Pan, J. Wu, Y. Bai, C. Xiao, X. Gao, J. Wang, N. Liu, MicroRNA-302s

Might Regulate ARL4C-Mediated Gastric Cancer Progression via p53 Signaling: Bioinformatics Analysis and Experiments Validation, Onco Targets Ther. 14 (2021) 2541-2553. 10.2147/ott.S282992.
[12] A. Harada, S. Matsumoto, Y. Yasumizu, K. Shojima, T. Akama, H. Eguchi, A. Kikuchi, Localization of KRAS downstream target ARL4C to invasive pseudopods accelerates pancreatic cancer cell invasion, Elife 10 (2021) e66721. 10.7554/eLife.66721.
[13] M. Arakaki, M. Ishikawa, T. Nakamura, T. Iwamoto, A. Yamada, E. Fukumoto, M. Saito, K. Otsu, H. Harada, Y. Yamada, S. Fukumoto, Role of epithelial-stem cell interactions during dental cell differentiation, J. Biol. Chem. 287 (2012) 10590-10601. 10.1074/jbc.M111.285874.
[14] S. Fujii, K. Nagata, S. Matsumoto, K.I. Kohashi, A. Kikuchi, Y. Oda, T. Kiyoshima, N. Wada, Wnt/β-catenin signaling, which is activated in odontomas, reduces Sema3A expression to regulate odontogenic epithelial cell proliferation and tooth germ development, Sci. Rep. 9 (2019) 4257. 10.1038/s41598-019-39686-1.
[15] S. Al Thamin, Y. Chiba, K. Yoshizaki, T. Tian, L. Jia, X. Wang, K. Saito, J. Li, A. Yamada, S. Fukumoto, Transcriptional regulation of the basic helix-loop-helix factor AmeloD during tooth development, J. Cell. Physiol. 236 (2021) 7533-7543. 10.1002/jcp.30389.
[16] L.K. McCauley, A.J. Koh, C.A. Beecher, Y. Cui, J.D. Decker, R.T. Franceschi, Effects of differentiation and transforming growth factor beta 1 on PTH/PTHrP receptor mRNA levels in MC3T3-E1 cells, J. Bone Miner. Res. 10 (1995) 1243-1255. 10.1002/jbmr.5650100815.
[17] T. Kiyoshima, H. Fujiwara, K. Nagata, H. Wada, Y.F. Ookuma, M. Shiotsuka, M. Kihara, K. Hasegawa, H. Someya, H. Sakai, Induction of dental epithelial cell differentiation marker gene expression in non-odontogenic human keratinocytes by transfection with thymosin beta 4, Stem Cell Res. 12 (2014) 309-322. 10.1016/j.scr.2013.11.006.
[18] R. Nagano, S. Fujii, K. Hasegawa, H. Maeda, T. Kiyoshima, Wnt signaling promotes tooth germ development through YAP1-TGF-β signaling, Biochem. Biophys. Res. Commun. 630 (2022) 64-70. 10.1016/j.bbrc.2022.09.012.
[19] X. Wang, Y. Chiba, L. Jia, K. Yoshizaki, K. Saito, A. Yamada, M. Qin, S. Fukumoto, Expression Patterns of Claudin Family Members During Tooth Development and the Role of Claudin-10 (Cldn10) in Cytodifferentiation of Stratum Intermedium, Front. Cell Dev. Biol. 8 (2020) 595593. 10.3389/fcell.2020.595593.
[20] Y. Chiba, K. Yoshizaki, T. Tian, K. Miyazaki, D. Martin, K. Saito, A. Yamada, S. Fukumoto, Integration of Single-Cell RNA- and CAGE-seq Reveals Tooth-Enriched

Genes, J. Dent. Res. 101 (2021) 220345211049785. 10.1177/00220345211049785.
[21] Y. Mikami, S. Fujii, K. Nagata, H. Wada, K. Hasegawa, M. Abe, R.U. Yoshimoto, S. Kawano, S. Nakamura, T. Kiyoshima, GLI-mediated Keratin 17 expression promotes tumor cell growth through the anti-apoptotic function in oral squamous cell carcinomas, J. Cancer Res. Clin. Oncol. 143 (2017) 1381-1393. 10.1007/s00432-017-2398-2.
[22] S. Fujii, T. Fujimoto, K. Hasegawa, R. Nagano, T. Ishibashi, K.J. Kurppa, Y. Mikami, M. Kokura, Y. Tajiri, T. Kibe, H. Wada, N. Wada, S. Kishida, Y. Higuchi, T. Kiyoshima, The Semaphorin 3A-AKT axis-mediated cell proliferation in salivary gland morphogenesis and adenoid cystic carcinoma pathogenesis, Pathol. Res. Pract. 236 (2022) 153991. 10.1016/j.prp.2022.153991.
[23] S. Fujii, Y. Tajiri, K. Hasegawa, S. Matsumoto, R.U. Yoshimoto, H. Wada, S. Kishida, M.A. Kido, H. Yoshikawa, S. Ozeki, T. Kiyoshima, The TRPV4-AKT axis promotes oral squamous cell carcinoma cell proliferation via CaMKII activation, Lab. Invest. 100 (2020) 311-323. 10.1038/s41374-019-0357-z.
[24] K. Hasegawa, S. Fujii, S. Matsumoto, Y. Tajiri, A. Kikuchi, T. Kiyoshima, YAP signaling induces PIEZO1 to promote oral squamous cell carcinoma cell proliferation, J. Pathol. 253 (2021) 80-93. 10.1002/path.5553.
[25] H. Miyoshi, U. Blomer, M. Takahashi, F.H. Gage, I.M. Verma, Development of a self-inactivating lentivirus vector, J. Virol. 72 (1998) 8150-8157. 10.1128/JVI.72.10.8150-8157.1998.
[26] A.M. Bolger, M. Lohse, B. Usadel, Trimmomatic: a flexible trimmer for Illumina sequence data, Bioinformatics 30 (2014) 2114-2120. 10.1093/bioinformatics/btu170.
[27] B. Li, C.N. Dewey, RSEM: accurate transcript quantification from RNA-Seq data with or without a reference genome, BMC Bioinformatics 12 (2011) 323. 10.1186/1471-2105-12-323.
[28] B. Langmead, S.L. Salzberg, Fast gapped-read alignment with Bowtie 2, Nat. Methods 9 (2012) 357-359. 10.1038/nmeth.1923.
[29] M.D. Robinson, D.J. McCarthy, G.K. Smyth, edgeR: a Bioconductor package for differential expression analysis of digital gene expression data, Bioinformatics 26 (2010) 139-140. 10.1093/bioinformatics/btp616.
[30] A. Subramanian, P. Tamayo, V.K. Mootha, S. Mukherjee, B.L. Ebert, M.A. Gillette, A. Paulovich, S.L. Pomeroy, T.R. Golub, E.S. Lander, J.P. Mesirov, Gene set enrichment analysis: a knowledge-based approach for interpreting genome-wide expression profiles, Proc. Natl. Acad. Sci. U. S. A. 102 (2005) 15545-15550. 10.1073/pnas.0506580102.
[31] F. Supek, M. Bošnjak, N. Škunca, T. Šmuc, REVIGO summarizes and visualizes long lists of gene ontology terms, PLoS One 6 (2011) e21800.

10.1371/journal.pone.0021800.
[32] Y. Mikami, S. Fujii, K.I. Kohashi, Y. Yamada, M. Moriyama, S. Kawano, S. Nakamura, Y. Oda, T. Kiyoshima, Low-grade myofibroblastic sarcoma arising in the tip of the tongue with intravascular invasion: A case report, Oncol. Lett. 16 (2018) 3889-3894. 10.3892/ol.2018.9115.
[33] K. Hasegawa, S. Fujii, K.J. Kurppa, T. Maehara, K. Oobu, S. Nakamura, T. Kiyoshima, Clear cell squamous cell carcinoma of the tongue exhibits characteristics as an undifferentiated squamous cell carcinoma, Pathol. Res. Pract. 235 (2022) 153909. 10.1016/j.prp.2022.153909.
[34] H. Kimura, K. Fumoto, K. Shojima, S. Nojima, Y. Osugi, H. Tomihara, H. Eguchi, Y. Shintani, H. Endo, M. Inoue, Y. Doki, M. Okumura, E. Morii, A. Kikuchi, CKAP4 is a Dickkopf1 receptor and is involved in tumor progression, J. Clin. Invest. 126 (2016) 2689-2705. 10.1172/JCI84658.
[35] H. Ji, L.I. Ehrlich, J. Seita, P. Murakami, A. Doi, P. Lindau, H. Lee, M.J. Aryee, R.A. Irizarry, K. Kim, D.J. Rossi, M.A. Inlay, T. Serwold, H. Karsunky, L. Ho, G.Q. Daley, I.L. Weissman, A.P. Feinberg, Comprehensive methylome map of lineage commitment from haematopoietic progenitors, Nature 467 (2010) 338-342. 10.1038/nature09367.
[36] H. Harada, P. Kettunen, H.S. Jung, T. Mustonen, Y.A. Wang, I. Thesleff, Localization of putative stem cells in dental epithelium and their association with Notch and FGF signaling, J. Cell Biol. 147 (1999) 105-120. 10.1083/jcb.147.1.105.
[37] I. Hofmann, A. Thompson, C.M. Sanderson, S. Munro, The Arl4 family of small G proteins can recruit the cytohesin Arf6 exchange factors to the plasma membrane, Curr. Biol. 17 (2007) 711-716. 10.1016/j.cub.2007.03.007.
[38] K. Nakashima, X. Zhou, G. Kunkel, Z. Zhang, J.M. Deng, R.R. Behringer, B. de Crombrugghe, The novel zinc finger-containing transcription factor osterix is required for osteoblast differentiation and bone formation, Cell 108 (2002) 17-29. 10.1016/s0092-8674(01)00622-5.
[39] J.M. Bae, J.C. Clarke, H. Rashid, M.D. Adhami, K. McCullough, J.S. Scott, H. Chen, K.M. Sinha, B. de Crombrugghe, A. Javed, Specificity Protein 7 Is Required for Proliferation and Differentiation of Ameloblasts and Odontoblasts, J. Bone Miner. Res. 33 (2018) 1126-1140. 10.1002/jbmr.3401.
[40] M.A. Nieto, Epithelial plasticity: a common theme in embryonic and cancer cells, Science 342 (2013) 1234850. 10.1126/science.1234850.

Figure Legends

Fig. 1. Arl4c expression in mouse tooth germ.

(**A**) E15 tooth germ rudiments were separated into the epithelium (epi) and the mesenchyme (mes). *Arl4c* mRNA levels were measured in the rudiments using quantitative RT-PCR. Relative *Cdh1*, *Vimentin* and *Arl4c* mRNA expression levels were normalized by *GAPDH* and expressed as fold-changes compared with levels in the epithelium. (**B**) Differential expression analysis of cell-type marker genes using Uniform Manifold Approximation and Projection (UMAP) visualization of single-cell datasets from P1 Krt14-RFP mouse molar (left panels) and P7 Krt14-RFP mouse incisor (right panels) were performed and *Arl4c* was detected in single-cell datasets (upper panels). Dot plot showed the expression of Arl-family across the cell cluster (lower panels). Am, ameloblast; Pre-am, pre-ameloblast; IEE, inner enamel epithelium; SI, stratum intermedium; SR-OEE, stellate reticulum-outer enamel epithelium; DP, dental pulp; Od, odontoblast; Sub-od, sub-odontobalstic layer; DF, dental follicle; PDL, periodontal ligament; Ery, erythrocyte; Leuko, leukocyte; Endo, endothelium; Peri, pericyte. Results are shown as means ± s.d. of three independent experiments. * $P<0.01$.

Fig. 2. The effects of ARNO inhibitor on tooth germ development.

(**A**) E15 tooth germ rudiments were cultured for 7 days. They were treated with or without 25 μM SecinH3, and then the culture medium was changed every second or third day with or without 25 μM SecinH3. The tooth germs were photographed just before fixing (phase-contrast images; left panels), then the size was measured (see Supplementary Fig. S2A) (right graph). Black dot lines indicate the outline of the tooth germ. (**B, C**) The rudiment sections were stained with H&E. The solid box represents the enlarged images (**B**). Tooth

area and thickness of the eosinophilic area (see Supplementary Fig. S2B) were evaluated (**C**). The arrows indicate the thickness of the eosinophilic area between ameloblast and odontoblast. Scale bars: 50 μm. Results are shown as means ± s.d. of three independent experiments. ** $P< 0.05$.

Fig. 3. Arl4c expression induces osteoblastic differentiation of odontogenic epithelial cells.

(**A**) Relative levels of *Arl4c* mRNA were normalized to *GAPDH* and expressed as fold-change compared with control cells. Lysates of mDE6 cells expressing control or Arl4c shRNA were probed with anti-Arl4c and anti-β-actin antibodies. (**B**) mDE6 expressing shControl or shArl4c were cultured in control medium (CM) or osteoblastic/ameloblastic differentiation medium (DM) for 4 weeks. Then the cells were fixed by 4% PFA and stained for ALZ (left panel), and then positive areas were calculated (right graph). (**C**) The red and blue dots in the volcano plot represent significantly upregulated or downregulated genes, respectively, in the mDE6 cells expressing shArl4c compared with mDE6 cells expressing shControl. Not differentially expressed genes (DEGs) are represented as grey dots. (**D**) Enrichment plot of "BONE MORPHOGENESIS", "OSSIFICATION" and "OSTEOBLAST DIFFERENTIATION" was shown using GSEA. (**E**) Relative gene expression of downregulated genes relating to bone mineralization, osteoblast differentiation, ossification, bone morphogenesis and positive regulation of cell proliferation (see Supplementary Fig. S4B) in mDE6 cells expressing control shRNA (white column) and Arl4c shRNA (black column) were measured using quantitative RT-PCR. Results are shown as means ± s.d. of three independent experiments. * $P< 0.01$. ** $P< 0.05$.

Figure 1

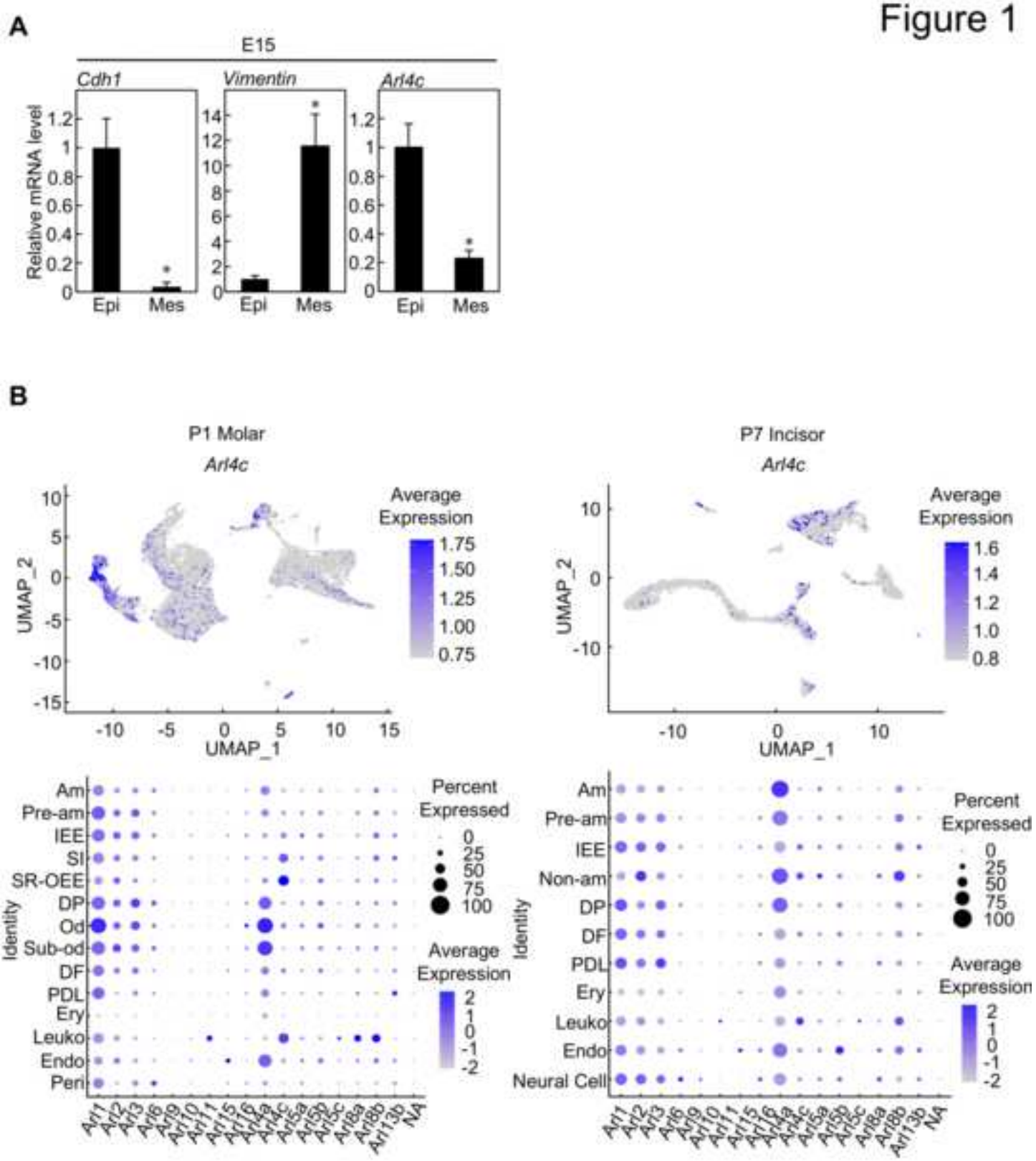

Figure 2

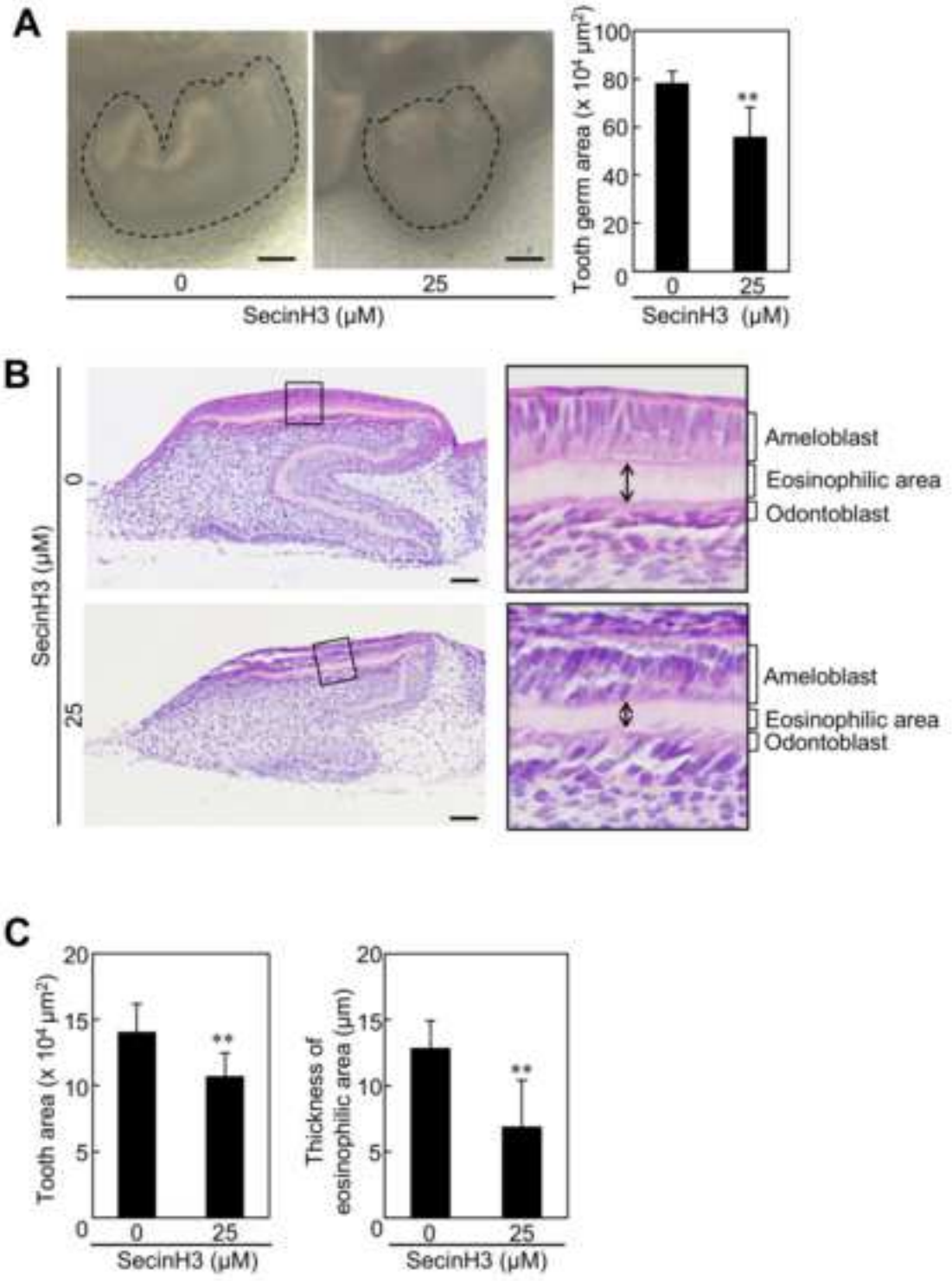

Figure 3

Click here to access/download;Figure;Fig3.tiff

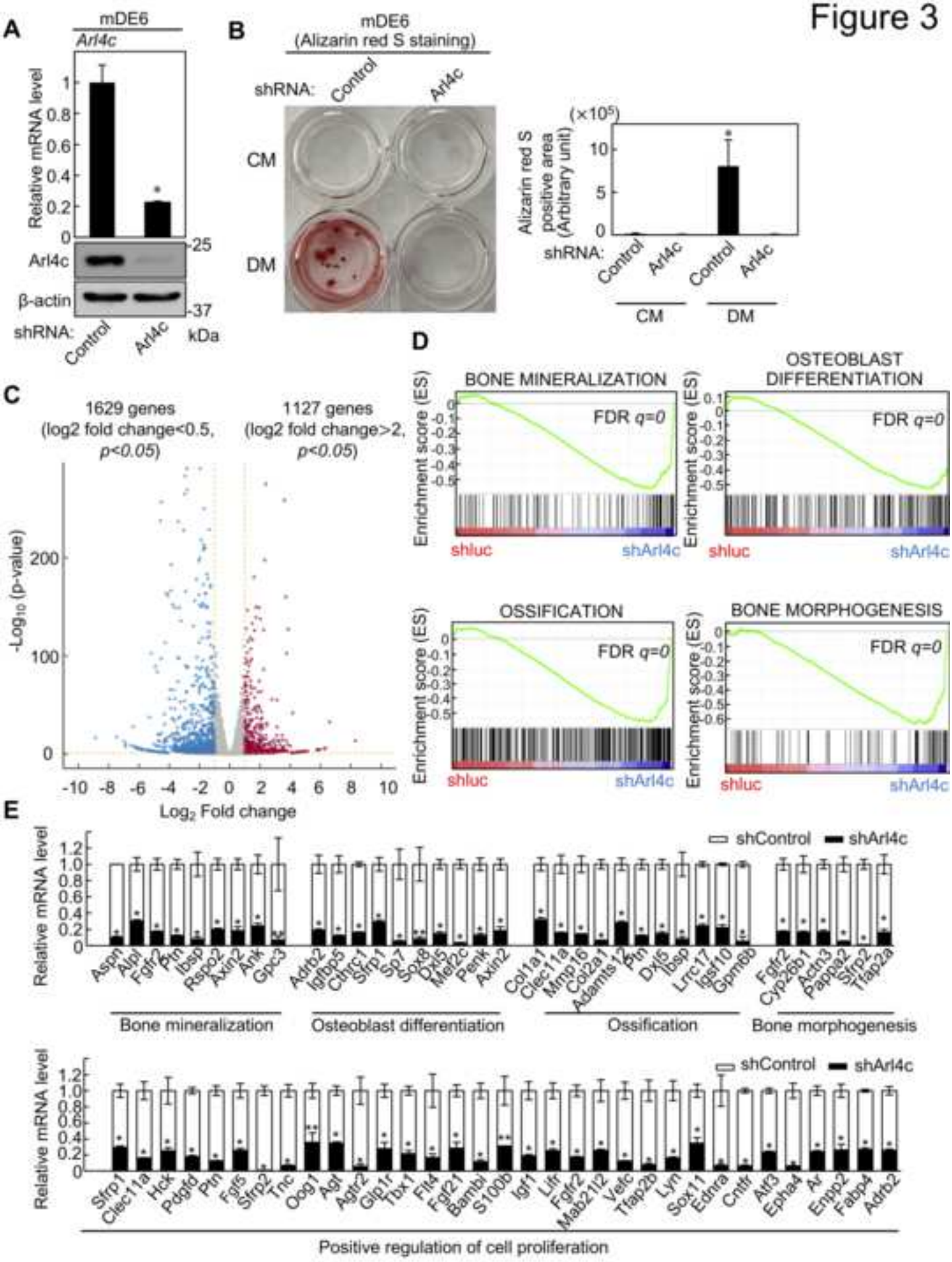

Declaration of competing interest

The authors declare that they have no known competing financial interests or personal relationships that could have appeared to influence the work reported in this paper.

mDE6

Figure S3A

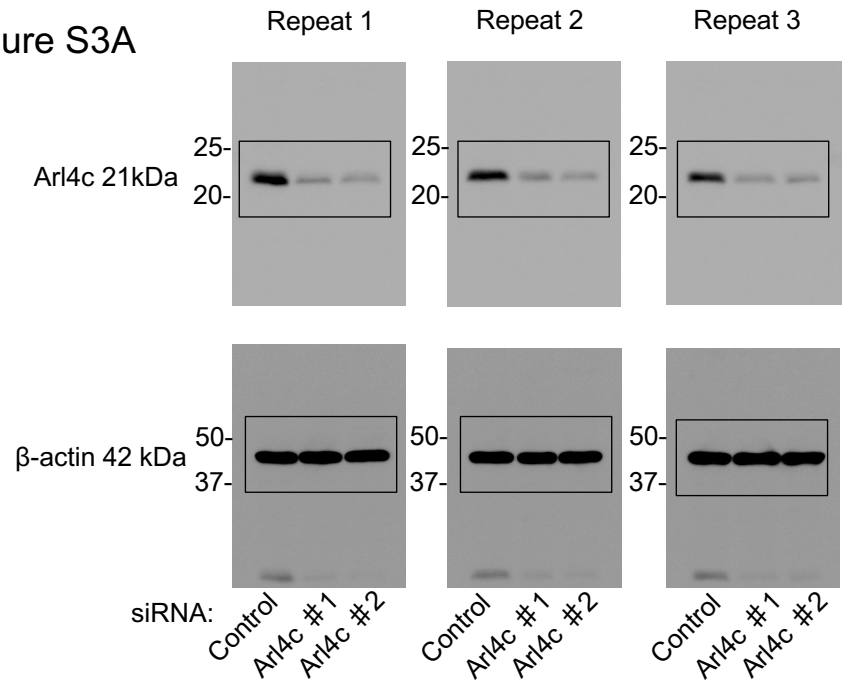

Figure S3B

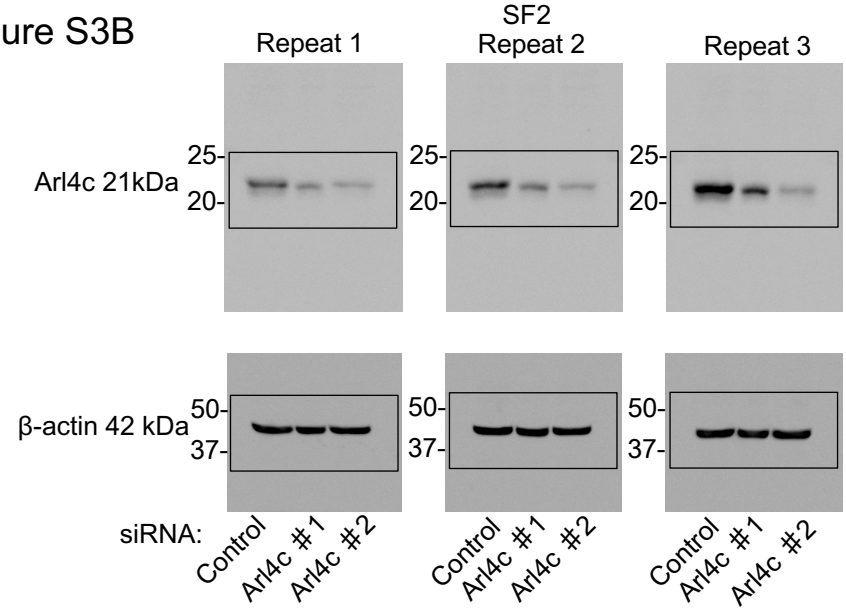

Figure 3A

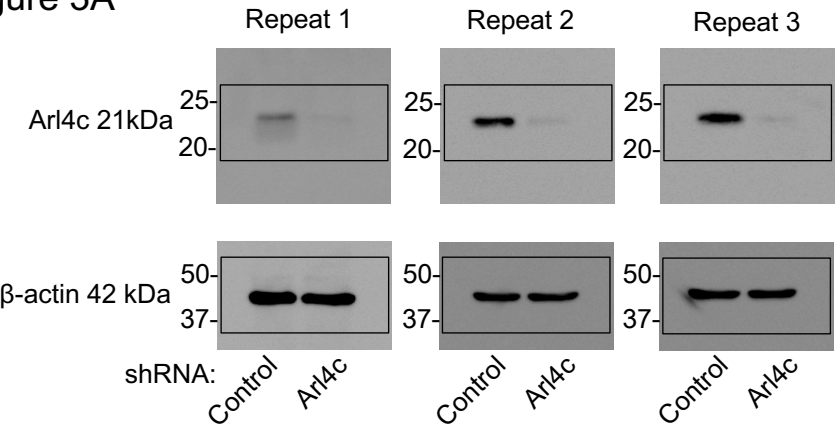

Full scan images of immunoblots presented in Figure S3A, B and Figure 3A.

Figure S3C

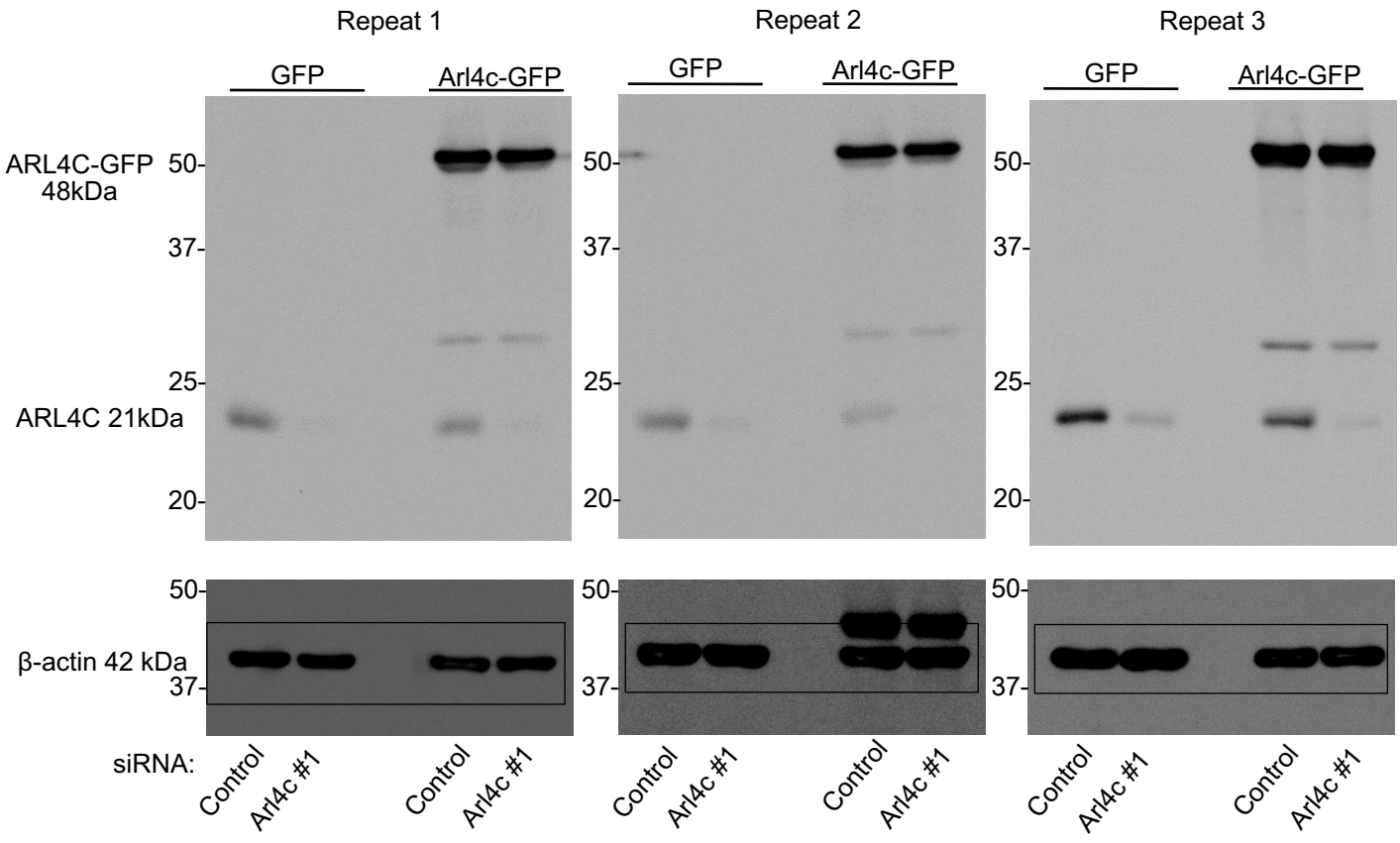

Figure S3D

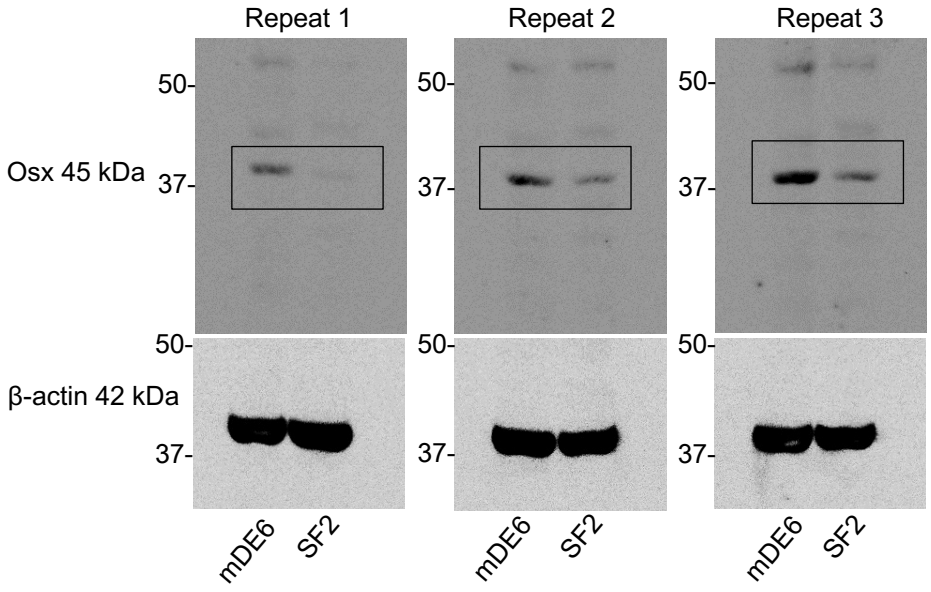

Full scan images of immunoblots presented in Figure S3C, D